

Preliminary Study on the Application of the PRAGMA/SPHINCS Code System to i-SMR Design

Seyeon Hwang, Jooil Yoon*

KEPCO International Nuclear Graduate School, 658-91 Haemaji-ro, Seosaeng-myeon, Ulju-gun, Ulsan 45014, Korea

*Corresponding author: jiyoon@kings.ac.kr

Keywords : i-SMR, PRAGMA/SPHINCS, Code system, Core analysis, Nuclear design

1. Introduction

The i-SMR (innovative Small Modular Reactor) provides significant operational advantages, including boron-free operation and extended refueling intervals of up to 24 months, enhancing reactor safety, operational flexibility, and economic efficiency. Due to its boron-free operational design, the i-SMR relies solely on control rods to regulate reactivity. For this reason, a new type of burnable absorber rod called HIGA (Highly Intensive and Discrete Gadolinia/Alumina Burnable Absorber)[1] has been designed. HIGA extends the self-shielding effect of gadolinium, facilitating prolonged reactivity flattening throughout the operating cycle. Achieving these operational targets requires highly accurate analytical tools and thorough validation of their predictive capabilities. This study presents a preliminary validation of an integrated computational approach that utilizes the PRAGMA (Power Reactor Analysis using GPU-based Monte Carlo Algorithm) [2] and SPHINCS[3] codes for detailed core analysis of the i-SMR.

In this study, we evaluate the accuracy and performance of the PRAGMA/SPHINCS code system based on the i-SMR design incorporating HIGA. In this system, PRAGMA generates precise microscopic cross sections homogenized at the pin level, thereby improving data fidelity over traditional methods. These cross sections serve as input for SPHINCS, a specialized pin-wise reactor core analysis code, which employs a pin-wise planar domain decomposition method accelerated by an assembly-level Coarse Mesh Finite Difference (CMFD) method to perform comprehensive 3D reactor core simulations. To validate the accuracy and reliability of the PRAGMA/SPHINCS coupled system, the calculation results are compared with a benchmark problem that utilized the KARMA/ASTRA code system.

2. Methodology

2.1 PRAGMA code

PRAGMA, developed by Seoul National University, is a continuous energy Monte Carlo code optimized for GPUs. It enhances computational efficiency through optimized cross-section lookup methods, vectorized

tracking algorithms, and acceleration techniques including Coarse Mesh Finite Difference (CMFD). For multigroup cross section generation, PRAGMA tallies reaction rates and neutron fluxes, derives pin-wise diffusion equations from the neutron transport equation by discretizing space, angle, and energy, and applies Legendre expansion to handle scattering effects. The code uses the P1 approximation to calculate diffusion coefficients and processes transport cross sections using a 47-group structure that is subsequently condensed. Through these advanced techniques, PRAGMA effectively handles complex particle simulations and typically produces results within 2 minutes.

2.2 SPHINCS code

SPHINCS is designed for pin-wise, two-step reactor core analysis. Based on diffusion theory, SPHINCS efficiently calculates 3D core distributions through a pin-level computational approach. Specifically, it utilizes a 2D-1D directional decoupling strategy, which separates radial (2D) and axial (1D) calculations to optimize computational performance while maintaining high accuracy. This method is implemented within a two-level CMFD framework. Figure 1 shows the calculation procedure for the 3D pin-wise analysis based on the 2D/1D decoupling with two-level CMFD acceleration.

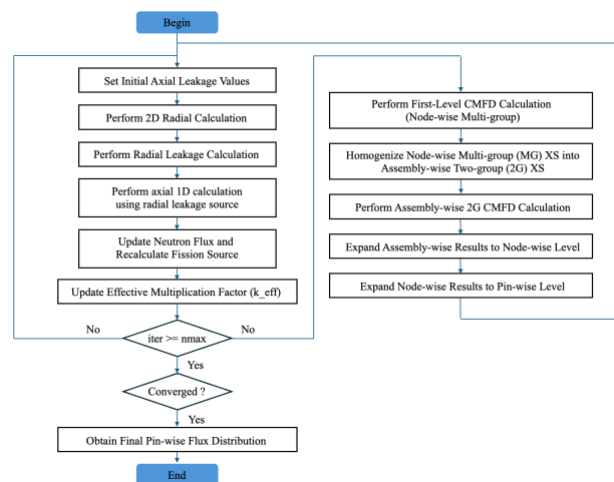


Fig. 1. Overall procedure of 3D pin-wise neutron diffusion calculation.

2.3 Coupling of PRAGMA and SPHINCS

The PRAGMA/SPHINCS code system is utilized for the reliable analysis of the i-SMR design. The procedure for this code system begins with the generation of pin-wise homogenized multi-group cross sections using the PRAGMA code. These cross sections are then converted into group constants and supplied as input files to SPHINCS. Subsequently, SPHINCS employs the provided cross section data to conduct a three-dimensional core calculation based on the pin-wise neutron diffusion equation. Figure 2 shows the flow chart of two-step neutronics calculation procedure.

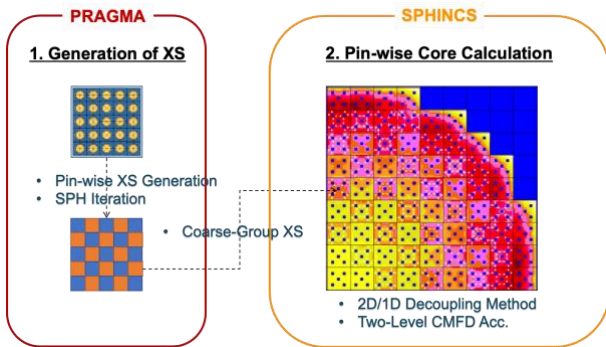


Fig. 2. Procedure of PRAGMA/SPHINCS code system.

3. Verification and Results

To verify the validity of the coupled calculations in the PRAGMA/SPHINCS code system, the i-SMR design utilized in the existing KARMA/ASTRA code system was selected as a benchmark. The i-SMR utilized as a benchmark in this study is designed with a core thermal power of 520 MWth (170 MWe). The reactor employs UO₂ fuel and utilizes standard nuclear fuel assemblies configured in a 17×17 arrangement, with a total of 69 fresh fuel bundles. The fuel concentration is limited to 5 wt% or less, and the refueling cycle is 24 months. Due to the soluble boron-free operation of SMRs, reactivity control is achieved using control rods, burnable absorber rods, and temperature variations in the moderator. The reactor system is fully passive to enhance reliability, and the overall design life is projected to be 80 years. The foundation of HIGA, designed for application in i-SMR, was developed based on a Discrete Burnable Absorber (Discrete BA) consisting of a sintered mixture with 10-20 mol% Gd₂O₃ content and the remainder as Al₂O₃. HIGA was designed in a form similar to conventional fuel rods to optimize its streamlined structure. Inside the standard cladding, the burnable absorber composed of Gd₂O₃ and Al₂O₃ is uniformly distributed in the form of sintered pellets.

Figure 3 represents a total of 16 different types of fuel assemblies were designed based on combinations

of IGD (Integral Gadolinia Burnable Absorber) fuel rods (4-26 rods, 1-8 wt% Gd₂O₃), and 16 HIGA rods (8-18 mol% Gd₂O₃). Before proceeding with the 3D pin-wise analysis, the multiplication factor versus burnup for all fuel assemblies are calculated using the PRAGMA as shown in figure 4. The results showed that assemblies composed solely of fuel rods, without burnable absorber rods, exhibited a linear decrease. In contrast, the H42 and I42 assembly, which contained relatively high concentrations of gadolinium at 8 wt% compared to other assemblies, displayed a bell-shaped distribution with symmetrical sides and a higher multiplication factor at the center. For the remaining assemblies, reactivity remained stable at the beginning of the cycle; however, towards the end of the cycle, it was observed that lower concentrations of gadolinium in the burnable absorber rod resulted in reduced reactivity duration.

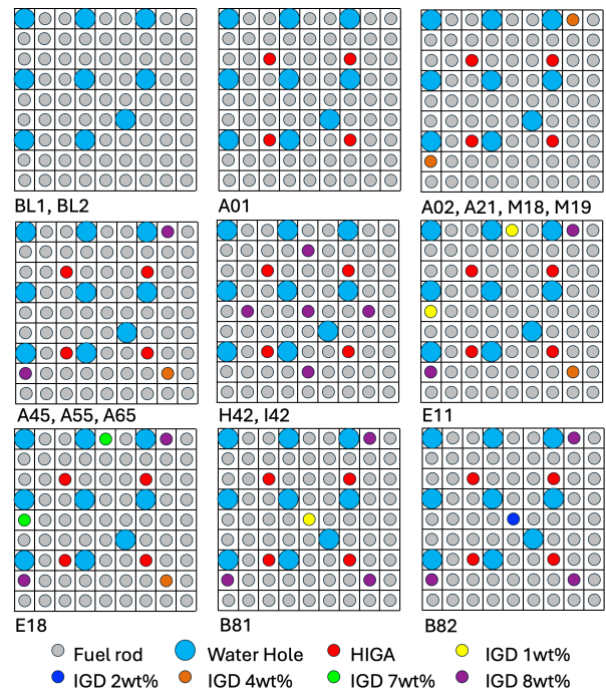


Fig. 3. Cross-sectional Views of 16 Types of Fuel Assemblies.

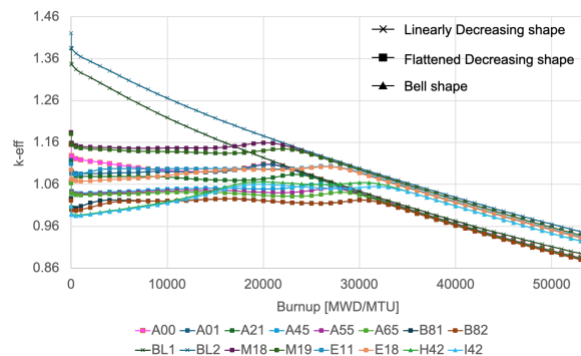


Fig. 4. Multiplication Factor by Fuel Assembly Type as a Function of Burnup for 16 Assembly Types.

The entire core was analyzed in 3D using the pin-wise homogenized cross-section data generated by the PRAGMA calculation. This analysis validated the reliability of the calculation by comparing it with the benchmark results from KARMA/ASTRA.

Figure 5 presents the reactor core design and control rod pattern of the i-SMR, which are primarily based on benchmark problems. To increase the stability of the i-SMR, a top-mounted Integral Control Instrumentation (ICI) system was implemented to prevent penetration below the core. And the control rods consist of four regulating bank group (R1, R2, R3, R4) and one shutdown bank group (SB). As the number of HIGA rods increase, the number of fuel rods decrease, ultimately leading to an increase in the average nominal power density of the fuel. To mitigate this issue, the number of HIGA rods is capped at 16, balancing the objectives of a 24-month cycle length and compliance with power peaking limits.

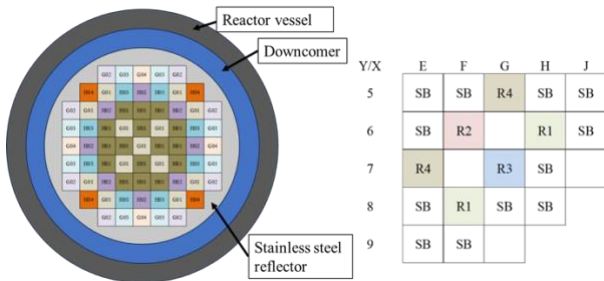


Fig. 5. SMR Core Design and Control Rod Loading Pattern.

Based on the i-SMR core design, there are a total of 8 types of fuel assemblies for first cycle, labeled A01 through A08. Each fuel assembly contains fuel rods that utilize U-235 at a concentration of 4%. The A01 assembly was deployed with HIGA composed of 10 mol% Gd₂O₃, while the A02 and A03 assemblies were deployed with HIGA containing 10 mol% and 12 mol% Gd₂O₃, respectively, as well as IGD with 3.5 wt% U-235 and 4 wt% Gd₂O₃. For assemblies A04 to A06, the Gd₂O₃ concentration within the HIGA was gradually increased from 12 mol% to 16 mol%, and the IGDs were categorized into two types: IGDs with 3.5 wt% U-235 and 4 wt% Gd₂O₃, and IGDs with 2.5 wt% U-235 and 8 wt% Gd₂O₃. Assemblies A07 and A08 utilized HIGA with 18 mol% Gd₂O₃, the highest concentration among the eight fuel assemblies, and IGDs with 3.95 wt% and 3.75 wt% U-235, along with 1 wt% and 2 wt% Gd₂O₃, respectively, as well as IGDs with 2.5 wt% U-235 and 8 wt% Gd₂O₃.

Figure 6 presents the core loading patterns, along with the axial assembly configurations utilized in Cycle 1. To optimize radial power distribution, highly reactive assemblies were strategically positioned in the peripheral area and a simple axial structure was designed for manufacturability.

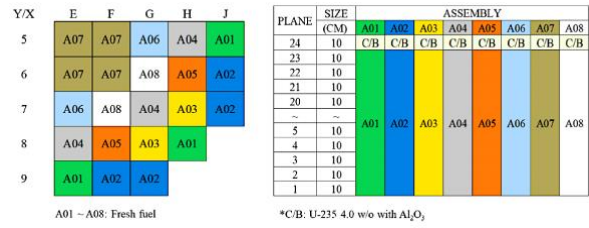


Fig. 6. Core Loading Pattern and Axial Assembly Configuration in Cycle 1.

Figure 7 represents the excess reactivity for the ARO (All Rod-Out) condition, expressed in EFPD (effective full power days). The graph indicate that the expected cycle length is approximately 830 EFPD, with the peak excess reactivity is around 1500 pcm. The reactivity swing is less than 600 pcm, indicating that the power remains uniformly maintained. Also, the result shows a difference of approximately 200 pcm when compared to the results obtained using the KARMA/ASTRA code. This discrepancy can be attributed to variations in the ENDF libraries. The KARMA/ASTRA code system utilizes ENDF/B-VI.8, whereas the PRAGMA/SPHINCS code system employs ENDF/B-VII.1.

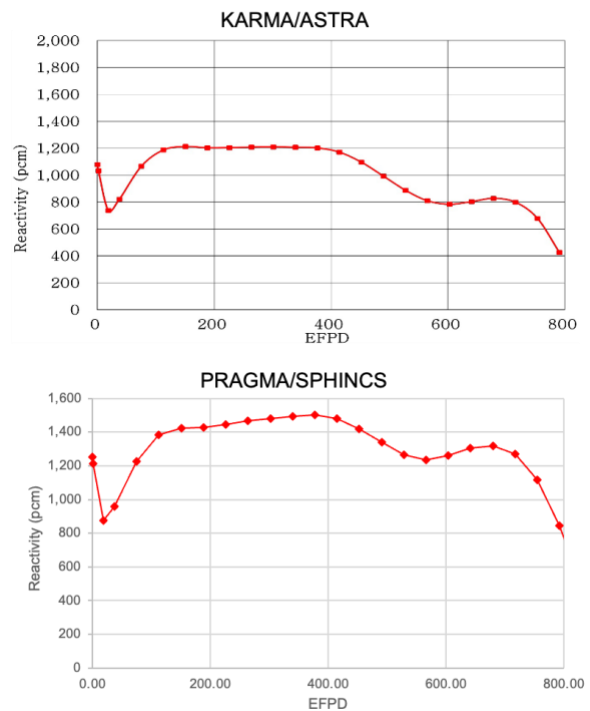


Fig. 7. Excess Reactivity Variation Curve under ARO Conditions in Cycle 1.

Figure 8 and Figure 9 represents the peaking factors and critical control rod positions of control banks with a 50% overlap of the regulating banks. The calculated cycle length is 21,000 MWD/MTU (approximately 790 EFPD) considering a 20% margin at the control rod position, which satisfies the required operating cycle (730 EFPD). The maximum Fr was determined to be

1.488, resulting in a uniform distribution of relative power per aggregate. The maximum Fq is 2.234, which is determined in conjunction with the axial peak power factor (Fz) value of approximately 1.4. At a power density of 3.86 kW/ft, the radially integrated 2D power density was calculated to be 5.744 kW/ft, while the maximum 3D power density was calculated to be 8.041 kW/ft. These values are lower than the typical target values for commercial PWRs, which are approximately 8.12 kW/ft (Fr = 1.45) and 13.61 kW/ft (Fq = 2.43), respectively.[4]

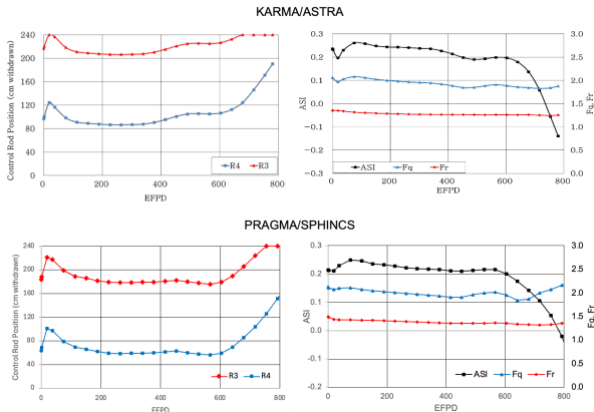


Fig. 8. Peaking factor and critical rod positions versus burnup in cycle 1.

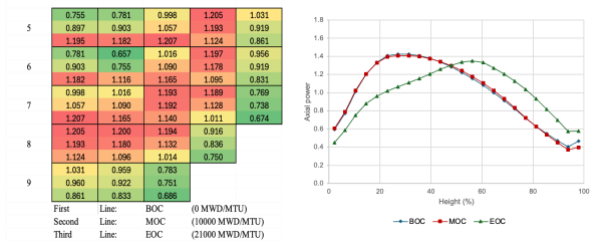


Fig. 9. Relative Power Distribution and Axial Power Distribution at BOC, MOC, and EOC in Cycle 1.

In the equilibrium cycle, a total of four types of fuel assemblies are utilized (X01, X02, X03, X04), incorporating a combination of 16 HIGA rods with Gd₂O₃ contents ranging from 9 mol% to 15 mol% and IGD rods with 3 wt% to 8 wt% Gd₂O₃. Figure 10 presents the core loading pattern of the core and the axial fuel rod configuration in the equilibrium cycle.

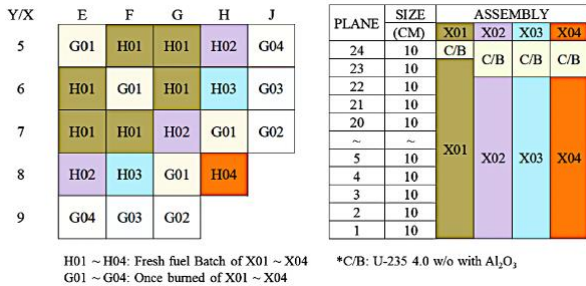


Fig. 10. Core Loading Pattern and Axial Assembly Configuration in the Equilibrium Cycle.

Figure 11 presents a flat reactivity trend, starting at 1800 pcm at the beginning of the cycle and decreasing to 1000 pcm by the end of the cycle, with a reactivity swing of about 500 pcm and an estimated cycle length of about 800 EFPD. Comparing the KARMA/ASTRA results, there is slightly difference in the excess reactivity. The reason is due to the inaccurate response of ASTRA to fuel loaded with both HIGA and IGD simultaneously, which affects the combustion behavior of Gd₂O₃.

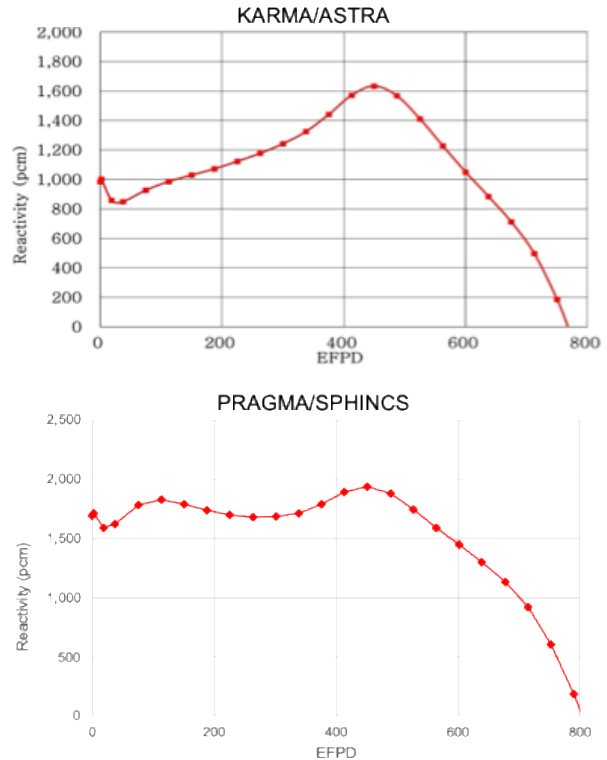


Fig. 11. Excess Reactivity Variation Curve of the Core under ARO Conditions in Equilibrium Cycle.

As shown in Figure 12, the ENDF difference results in a higher response compared to the KARMA/ASTRA calculation, as indicated in the previous cycle 1. Consequently, the control rod was operated with more control rod inserted. Additionally, due to the difference in ARO combustion behavior, the rod position differs depending on the combustion section. The fq value ranges from 2.0 to 2.5, while the fr is maintained at approximately 1.5. In comparison to cycle 1, the fr tends to be slightly higher due to the increased variation in rod position throughout combustion in the SPHINCS calculation. Although the ASI shows slight differences attributed to the rod position variations, the overall trend seems similar. Additionally, compared to the values of the cycle 1, the power distribution among the assemblies is skewed towards the H01 assemblies at the EOC as shown in Fig. 13.

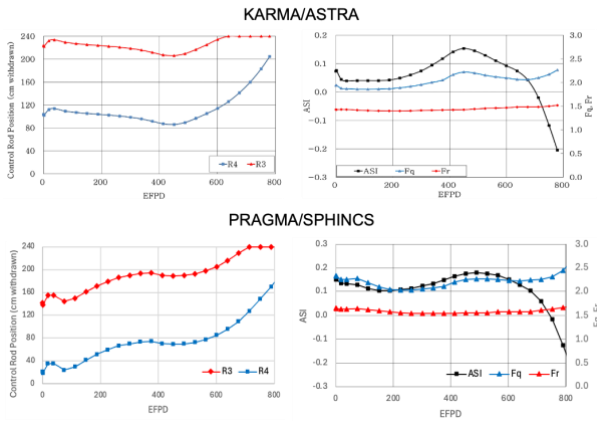


Fig. 12. Peaking factor and critical rod positions versus burnup in equilibrium cycle.

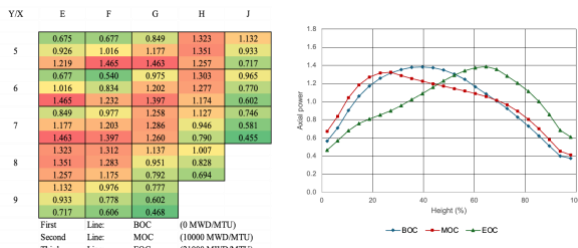


Fig. 13. Relative Power Distribution and Axial Power Distribution at BOC, MOC, and EOC in Equilibrium Cycle.

The i-SMR core depletion analysis covers 24 burnup points up to 20,000 MWD/MTU, utilizing the Semi Predictor-Corrector method below 100 MWD/MTU and the Full Predictor-Corrector method above this threshold. The calculations were performed on a MacBook M3 Max (4.05 GHz, 16 cores, and 64 GB RAM) using parallel computation with 1, 2, 4 and 8 CPU cores. Table 1 shows the number of iterations and the computational times for each stage of the calculations.

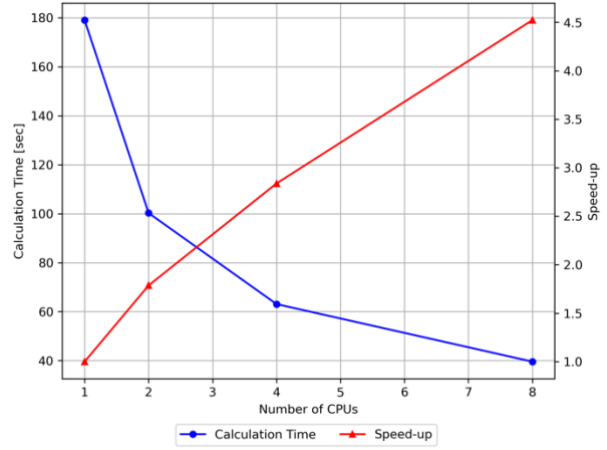
Table 1: Calculation performance at each depletion step in the i-SMR 3D problem

Burnup (MWD/d)	Depletion Type	# of 2D/1D Pin Calc.	CMFD Iteration	Time with 1 CPU (s)	Time with 2 CPUs (s)	Time with 4 CPUs (s)	Time with 8 CPUs (s)
0		47	250	5.77	3.19	1.98	1.29
50	SEMI	33	150	4.25	2.37	1.48	0.97
500	FULL	64	300	8.68	4.85	3.06	1.91
1000	FULL	64	300	8.70	4.81	3.06	1.91
2000	FULL	64	300	8.73	4.89	3.02	1.88
3000	FULL	62	300	8.32	4.71	2.93	1.86
4000	FULL	56	200	7.56	4.21	2.62	1.65
5000	FULL	56	200	7.49	4.14	2.64	1.67
6000	FULL	56	200	7.53	4.22	2.62	1.65
7000	FULL	56	200	7.58	4.22	2.67	1.63
8000	FULL	54	200	7.26	4.08	2.53	1.60
9000	FULL	56	200	7.48	4.24	2.62	1.64
10000	FULL	56	200	7.47	4.25	2.63	1.64
11000	FULL	63	300	8.39	4.75	2.97	1.88
12000	FULL	64	300	8.50	4.73	3.04	1.90
13000	FULL	64	300	8.51	4.73	3.06	1.91
14000	FULL	64	300	8.53	4.77	3.06	1.91
15000	FULL	60	300	8.12	4.58	2.91	1.82
16000	FULL	59	300	8.06	4.56	2.88	1.80
17000	FULL	56	200	7.66	4.30	2.68	1.65
18000	FULL	56	200	7.46	4.13	2.63	1.63
19000	FULL	64	300	8.48	4.76	3.02	1.89
20000	FULL	64	300	8.50	4.76	3.00	1.91
Total Time (s)				179.03	100.26	63.09	39.59

Figure 14 shows the computational time and relative performance improvement as a function of number of CPUs used in the calculation. The baseline calculation for i-SMR core analysis takes 180 seconds on a single

CPU core, but when using 8 CPUs in parallel, the calculation time is reduced to 40 seconds, resulting in a 4.5× performance improvement.

Fig. 14. Total calculation time and relative speed-up in the i-SMR 3D problem



4. Conclusion

The PRAGMA/SPHINCS code system is a coupled code system for the reliable analysis of i-SMR designs. PRAGMA and SPHINCS are coupled to perform neutron transport analysis within the reactor core. The PRAGMA code performs probabilistic neutron transport calculations for individual fuel pins, generating multi-group neutron cross sections. These cross sections are subsequently converted into group constants and input into SPHINCS. In turn, SPHINCS utilizes the provided neutron cross section data to perform 3D reactor core calculations based on the pin-wise neutron diffusion equation. This process allows for the interpretation of neutron behavior within the reactor and the evaluation of the nuclear design of the i-SMR.

In this study, the i-SMR design using HIGA was re-evaluated using the PRAGMA/SPHINCS code and compared to the existing KARMA/ASTRA results. The results showed an excess reactivity difference of approximately 300 pcm in the cycle 1 ARO condition and up to 700 pcm in the equilibrium cycle ARO condition. This difference is likely attributed to differences in the ENDF libraries utilized by each code and inaccuracies in the combustion capabilities of the HIGA/IGD burnable absorber rods.

The comparative analysis demonstrated strong agreement, affirming the suitability and accuracy of the PRAGMA/SPHINCS integrated code system for advanced core design and analysis of i-SMR reactors. Future research will focus on improving the accuracy and speed of PRAGMA/SPHINCS, aiming to explore more precise calculation methods for i-SMR with boron-free operational characteristics.

ACKNOWLEDGEMENT

This work was supported by the 2025 Research Fund of the KEPCO International Nuclear Graduate School(KINGS), Republic of Korea.

REFERENCES

- [1] J. S. Kim, T. S. Jung, J. I. Yoon, Reactor core design with practical gadolinia burnable absorbers for soluble boron-free operation in the innovative SMR, Nuclear Engineering and Technology, Vol.56, p.3144-3154, 2024
- [2] N. Choi, K. M. Kim, H. G. Joo, Domain Decomposition for GPU-Based Continuous Energy Monte Carlo Power Reactor Calculation, Nuclear Engineering and Technology, Vol.52, p.2667-2668, 2020
- [3] J. I. Yoon, H. C. Lee, H. G. Joo, H. S. Kim, High performance 3D pin-by-pin neutron diffusion calculation based on 2D/1D decoupling method for accurate pin power estimation, Nuclear Engineering and Technology, Vol.53, p.3543-3562, 2021
- [4] APR1400 Design Control Document Tier2, KHNP, APR1400-K-X-FS-14002-NP, Revision 3, 2018